21. Materials and methods are available as supporting material on *Science* Online.
22. N. Shakhova, I. Semiletov, G. Panteleev, *Geophys. Res. Lett.* **32**, L09601 (2005).
23. N. Shakhova, I. Semiletov, *J. Mar. Syst.* **66**, 227 (2007).
24. All the seawater-dissolved CH_4 concentration data are publicly and freely available at http://research.iarc.uaf.edu/SSSS/. A description of this large database as compared with previous ocean CH_4 studies is presented in table S3.
25. W. S. Reeburgh, *Chem. Rev.* **107**, 486 (2007).
26. I. Leifer, B. Luyendyk, J. Boles, J. Clark, *Global Biogeochem. Cycles* **20**, GB3008 (2006).
27. N. J. P. Owens, C. S. Law, R. F. C. Mantoura, P. H. Burkill, C. A. Llewellyn, *Nature* **354**, 293 (1991).
28. D. M. Karl *et al.*, *Nat. Geosci.* **1**, 473 (2008).
29. G. K. Westbrook *et al.*, *Geophys. Res. Lett.* **36**, L15608 (2009).
30. LSMM closest to the study area is established for the Barrow, Alaska, USA, monitoring station at 71° 19′ N, 156° 35′ W (www.cmdl.noaa.gov/ccgg/insitu.html); it is equal to 1.85 ppmv.
31. The division into two subpopulations for background and hotspot areas within the ESAS was based on a statistical approach detailed in SOM text S2.1 and displayed graphically in fig. S4. These two resolved populations were then first subjected to an empirical distribution function (EDF) test (SOM text S1.1). The results of the EDF test (table S1) yielded that a lognormal distribution function best fit the data. This function was hence used when applying the maximum likelihood (ML) method to calculate the statistical population parameters mean and variance [expressed as upper and lower 95% confidence limits (equations are provided in SOM text S1.1)]. The derived population parameters, displayed in table S2, were then used to estimate the overall ESAS CH_4 fluxes as summarized in Table 1.
32. R. Wanninkhof, *J. Geophys. Res.* **97** (C5), 7373 (1992).
33. D. D. Baldocchi, *Glob. Change Biol.* **9**, 479 (2003).
34. J. B. Edson, A. A. Hinton, K. E. Prada, J. E. Hare, C. W. Fairall, *J. Atmos. Ocean. Technol.* **15**, 547 (1998).
35. T. Fujitani, *Pap. Meteorol. Geophys.* **36**, 157 (1985).
36. We thank V. Sergienko, G. Golitsyn, S. Akasofu, L. Hinzman, and V. Akulichev for their support of our work in the Siberian Arctic. This research was supported by the International Arctic Research Centre through a National Oceanic and Atmospheric Administration Cooperative Agreement, the Far Eastern Branch of the Russian Academy of Sciences, the Russian Foundation for Basic Research, NSF, the Swedish Research Council, and the Knut and Alice Wallenberg Foundation.

Supporting Online Material

www.sciencemag.org/cgi/content/full/327/5970/1246/DC1
Materials and Methods
SOM Text
Figs. S1 to S4
Tables S1 to S3
References

21 September 2009; accepted 21 January 2010
10.1126/science.1182221

Hippocampal Short- and Long-Term Plasticity Are Not Modulated by Astrocyte Ca^{2+} Signaling

Cendra Agulhon,[1]* Todd A. Fiacco,[2] Ken D. McCarthy[1]

The concept that astrocytes release neuroactive molecules (gliotransmitters) to affect synaptic transmission has been a paradigm shift in neuroscience research over the past decade. This concept suggests that astrocytes, together with pre- and postsynaptic neuronal elements, make up a functional synapse. Astrocyte release of gliotransmitters (for example, glutamate and adenosine triphosphate) is generally accepted to be a Ca^{2+}-dependent process. We used two mouse lines to either selectively increase or obliterate astrocytic G_q G protein–coupled receptor Ca^{2+} signaling to further test the hypothesis that astrocytes release gliotransmitters in a Ca^{2+}-dependent manner to affect synaptic transmission. Neither increasing nor obliterating astrocytic Ca^{2+} fluxes affects spontaneous and evoked excitatory synaptic transmission or synaptic plasticity. Our findings suggest that, at least in the hippocampus, the mechanisms of gliotransmission need to be reconsidered.

Calcium transients in astrocytes are physiologically driven by metabotropic G_q G protein–coupled receptors (G_q GPCRs), which can be activated after neurotransmitter release from presynaptic terminals (*1*, *2*). At Schaffer collateral-CA1 (SC-CA1) synapses in acute hippocampal slices, astrocytes can modulate neuronal activity by elevations in Ca^{2+} that are evoked by the following: (i) uncaging IP_3 or Ca^{2+} in individual astrocytes, (ii) repetitive depolarization of the astrocyte membrane, (iii) mechanical stimulation of an astrocyte, or (iv) bath application of endogenous G_q GPCR agonists. With these pharmacological approaches, astrocyte Ca^{2+} elevations have been reported to trigger gliotransmitter release from astrocytes, resulting in the modulation of synaptic transmission and plasticity through the activation of presynaptic [for example, group I metabotropic glutamate receptors (mGluRs) or adenosine A(1) receptors (A_1Rs)] or postsynaptic receptors [*N*-methyl-D-aspartate receptors (NMDARs)] (*3*–*11*). To circumvent a number of caveats associated with the pharmacological approaches described above (*12*–*15*), we have recently developed and characterized two genetically modified mice [the MrgA1$^+$ and IP_3R2 knockout (KO) mice] that enable either selective activation or inactivation of G_q GPCR Ca^{2+} signaling in astrocytes (*13*, *16*, *17*). Within the hippocampus, the stimulation of transgenic MrgA1 G_q GPCRs leads to astrocyte-specific Ca^{2+} responses that mimic the "Ca^{2+} fingerprint" response that is elicited by endogenous G_q GPCRs (*13*). In hippocampal slices derived from IP_3R2 KO mice (*17*), G_q GPCR Ca^{2+} signaling is obliterated selectively in 100% of astrocytes without affecting neuronal Ca^{2+} responses (*16*).

We first tested the possibility that astrocytic G_q GPCR Ca^{2+} is involved in the modulation of spontaneous excitatory postsynaptic currents (sEPSCs). In these and the following experiments, a high percentage of astrocytes (~90 to 100%) were stimulated so that each CA1 neuron has the vast majority of its synapses embedded in astrocyte processes that elevate Ca^{2+} upon G_q GPCR agonist application. Control experiments showed that MrgA1R expression by itself in astrocytes does not affect basal neuronal activity in a nonspecific manner [supporting online material (SOM) text S1]. MrgA1R agonist Phe-Met-Arg-Phe-NH_2 amide (FMRF, 15 μM) was applied to trigger Ca^{2+} elevations in ~90% of mature MrgA1$^+$ passive astrocytes (*13*) in cell bodies as well as fine processes (Fig. 1, A and B, boxes/traces 1 to 5, SOM text S2, and movie S1). No significant effect of astrocyte Ca^{2+} elevations on sEPSC frequency and amplitude in CA1 neurons from MrgA1$^+$ mice was found (Fig. 1C and SOM text S3, $n = 7$, $P > 0.05$). To test the possibility that this lack of effect might be caused by the stimulation of a transgenic G_q GPCR, we also stimulated endogenous astrocytic endothelin G_q GPCRs (ETRs), which were selected as optimal candidates because they evoke gliotransmitter release in vitro (*18*), they are thought to be very weakly expressed by neurons and heavily expressed by brain astrocytes at postnatal day 1 to 30 (*19*), and no direct effects on neuronal activity have been reported when stimulating ETRs (*13*). Astrocytic ETR-mediated Ca^{2+} increases in ~100% of astrocytes from wild-type (WT) hippocampal slices [endothelin 1 (ET1) and ET3, 10 nM each; SOM text S4, and fig. S1) had no effect on the frequency or amplitude of sEPSCs (Fig. 1, D to F, and SOM text S5, $n = 5$, $P > 0.05$).

Previous studies using conventional pharmacological approaches have suggested that postsynaptic NMDARs might be preferential targets for glutamate release from astrocytes (*3*–*7*, *9*, *10*), prompting us to examine the possibility that astrocytic G_q GPCR Ca^{2+} elevations modulate the NMDAR-mediated component of evoked whole-cell EPSCs (eEPSCs). FMRF does not produce a nonspecific effect on NMDA eEPSCs (Fig. 2, A and A1, and SOM text S6). FMRF or ETs were

[1]Department of Pharmacology, University of North Carolina at Chapel Hill, Genetic Medicine Building, CB 7365, Chapel Hill, NC 27599, USA. [2]Department of Cell Biology and Neuroscience, University of California Riverside, Riverside, CA 92521, USA.

*To whom correspondence should be addressed. E-mail: cendra_agulhon@med.unc.edu

applied to MrgA1$^+$ or WT slices, respectively, and the amplitude of NMDA eEPSCs was unaffected during agonist-mediated Ca^{2+} increases in astrocytes (Fig. 2, B and B1, and SOM text S7, MrgA1$^+$, $n = 11$, $P > 0.05$; Fig. 2, C and C1, and SOM text S7, WT, $n = 7$, $P > 0.05$).

Uncaging IP_3 or Ca^{2+} in astrocytes produces a transient enhancement of the probability of neurotransmitter release at a fraction of the SC terminals (*10*, *20*). We directly tested whether activating or inactivating astrocytic G_q GPCR Ca^{2+} signaling affects presynaptic release probability and short-term plasticity by measuring the paired-pulse facilitation (PPF) index of evoked field potentials (fEPSPs). Astrocytic MrgA1R expression by itself did not have a nonspecific effect on PPF (Fig. 2D and SOM text S8). No overall PPF profile changes were observed in association with astrocyte MrgA1R- or ETR-mediated Ca^{2+} elevations in MrgA1$^+$ or WT slices, respectively (Fig. 2E, MrgA1$^+$, $n = 7$, $P > 0.05$; Fig. 2F, WT, $n = 6$, $P > 0.05$). We reasoned that if astrocytic Ca^{2+} elevations regulate gliotransmitter release, then the removal of astrocytic G_q GPCR Ca^{2+} signaling should affect tonic and activity-induced gliotransmitter release and, consequently, PPF. Therefore, PPF was measured in IP_3R2 KO mice versus WT littermate controls. Again, no changes in PPF profiles were observed between the two groups (Fig. 2G, IP_3R2 KO, $n = 9$; WT, $n = 9$; $P = 0.73$).

A recent study has shown that temporal coincidence of astrocyte Ca^{2+} elevations (evoked by Ca^{2+} uncaging) and transient depolarization of CA1 neurons can induce a presynaptic form of long-term potentiation (LTP) in SC-CA1 synapses (*10*). Therefore, stimulating astrocytic G_q GPCR Ca^{2+} signaling simultaneously with depolarization of large ensembles of CA1 neurons should either directly induce LTP or at least modulate the baseline slope of fEPSPs through gliotransmitter activation of presynaptic group I mGluRs, or, alternatively, A_1Rs (*10*, *21*). Our data do not support these predictions (fig. S2, B, B1, C, C1, and SOM text S9).

We also directly tested whether astrocytic G_q GPCRs regulate LTP magnitude as well as post-tetanic potentiation (PTP). Similar to PPF, PTP is a form of short-term plasticity (*22*). First, a battery of control experiments clearly demonstrated that neither the selective astrocytic expression of MrgA1Rs nor the application of FMRF to WT slices affected input-output (I/O) curves, PTP, or LTP (Fig. 3, A and D, and SOM text S10). A prerequisite for the involvement of astrocytes in LTP is that their activation precedes the induction of LTP. After establishing a 15-min baseline recording of fEPSPs, Ca^{2+} elevations in astrocytes were induced by bath application of either FMRF to MrgA1$^+$ slices or ETs to WT slices. LTP was induced ~2.5 min after agonist application, when the peaks of Ca^{2+} responses in astrocytes reached their maximum (Fig. 3, B and C). LTP magnitudes obtained from MrgA1$^+$ slices

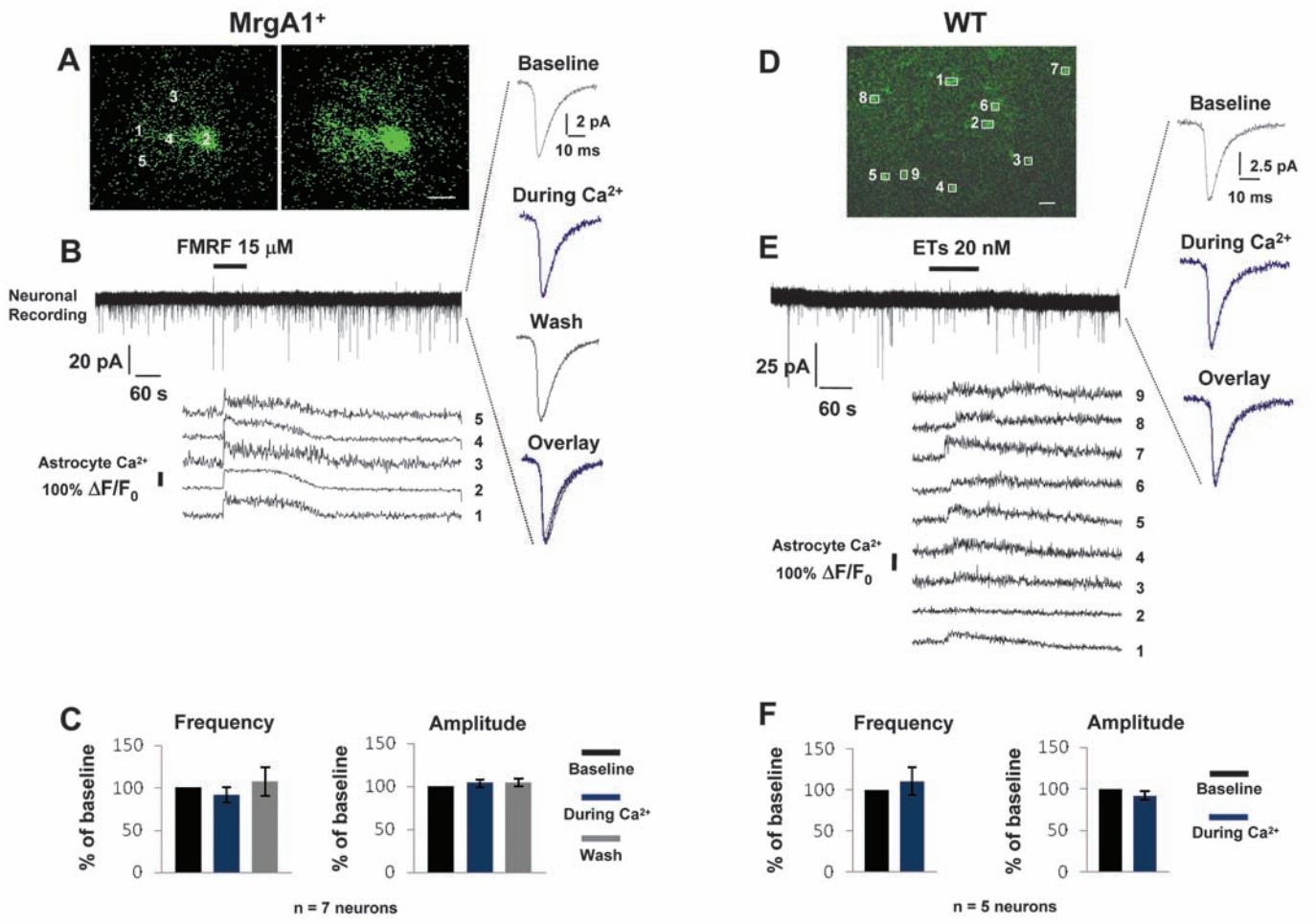

Fig. 1. Stimulation of astrocytic G_q GPCRs does not affect sEPSCs in CA1 pyramidal neurons. (**A**) Typical MrgA1$^+$ astrocyte in stratum radiatum (s.r.), filled with Oregon-Green-BAPTA-1 (OGB1), before (left) and after (right) stimulation of MrgA1Rs with FMRF (15 μM). Astrocyte Ca^{2+} responses are included as representative responses of the ~90% of responsive astrocytes within the slice and were used to monitor the beginning of Ca^{2+} elevations relative to neuronal activity. (**B** and **C**) sEPSCs frequency and amplitude remain unchanged [(B), upper] during astrocyte Ca^{2+} increases [(B), traces 1 to 5]. To the right are the averaged sEPSCs from the trace in (B). (**D**) Astrocytes (1 to 9) bulk-loaded with Ca^{2+} green 1-AM in s.r. from WT slices. (**E** and **F**) sEPSCs frequency and amplitude were unchanged during astrocyte ETR-mediated Ca^{2+} increases (ET1 and ET3, 10 nM each). Due to long-tailing ETR Ca^{2+} increases, sEPSCs were analyzed only during the first 120 s of astrocyte Ca^{2+} increases. Scale bars in (A) and (D) indicate 10 and 20 μm, respectively. Error bars indicate SEM.

stimulated with FMRF (137.97 ± 5.58%, $n = 14$ slices) or WT slices stimulated with ETs (133.13 ± 7.62%, $n = 9$), respectively, were no different from LTP magnitudes obtained in matching controls (Fig. 3, E and F, and SOM text S11, $P > 0.05$). Furthermore, PTP was also not affected (Fig. 3, E and F, and SOM text S11, $P > 0.05$).

Next, we examined whether the obliteration of astrocytic G_q GPCR Ca^{2+} signaling would affect basal synaptic transmission as well as PTP and LTP. No significant difference was found in I/O curves performed in IP_3R2 KO versus WT littermate control mice (Fig. 3G, IP_3R2 KO, $n = 21$; WT, $n = 18$; $P = 0.94$). These results indicate that both the pre- and postsynaptic responses, and thus the basal SC-evoked synaptic transmission, are intact in IP_3R2 KO mice, even though astrocytes are completely incapable of producing G_q GPCR Ca^{2+} elevations. No significant alteration in PTP and LTP was detected between IP_3R2 KO and control mice, demonstrating that astrocytic G_q GPCR–mediated Ca^{2+} signaling does not account for a tonic form nor an activity-induced form of short- and long-term synaptic plasticity (Fig. 3H and SOM text S12, IP_3R2 KO, $n = 10$; WT, $n = 8$, $P > 0.05$). To validate these IP_3R2 KO data, we showed that the LTP stimulation protocol used is sufficient to induce Ca^{2+} increases in astrocytes from WT slices (fig. S3). Finally, we also found that stimulating or removing astrocytic G_q GPCR Ca^{2+} signaling in $MrgA1^+$ or IP_3R2 KO mice, respectively, does not significantly alter LTP and PTP induced by theta-burst stimulation (SOM text S13).

Previous studies have demonstrated that activation of synaptic group I mGluRs, A_1Rs, or NMDARs depotentiates LTP at SC-CA1 synapses (*23*–*27*). These three receptors have all been reported to be the targets of astrocytic Ca^{2+}-dependent sources of glutamate or adenosine triphosphate (ATP)/adenosine under certain conditions (*12*). To further test whether astrocytic G_q GPCR Ca^{2+} signaling is sufficient to induce gliotransmitter release to affect synaptic transmission through the activation of synaptic mGluRs, A_1Rs, or NMDARs, we investigated the role of astrocyte Ca^{2+} signaling in the maintenance of LTP. Fifty minutes after LTP induction, astrocyte Ca^{2+} increases were elicited by applications of FMRF to $MrgA1^+$ slices or of ETs to WT slices. This did not lead to a significant change in the slope of fEPSPs (Fig. 4, A, B, and D, and SOM text S14, $n = 9$ $MrgA1^+$ slices, $n = 16$ WT slices, $P > 0.05$). As a positive control for agonist-induced depotentiation, we applied (RS)-3,5-dihydroxyphenylglycine (DHPG, 50 μM), which exerted a significant depotentiation of the slope in all slices tested (Fig. 4, A and D; $MrgA1^+$, 74.82 ± 3.45%, $n = 12$, $P <$

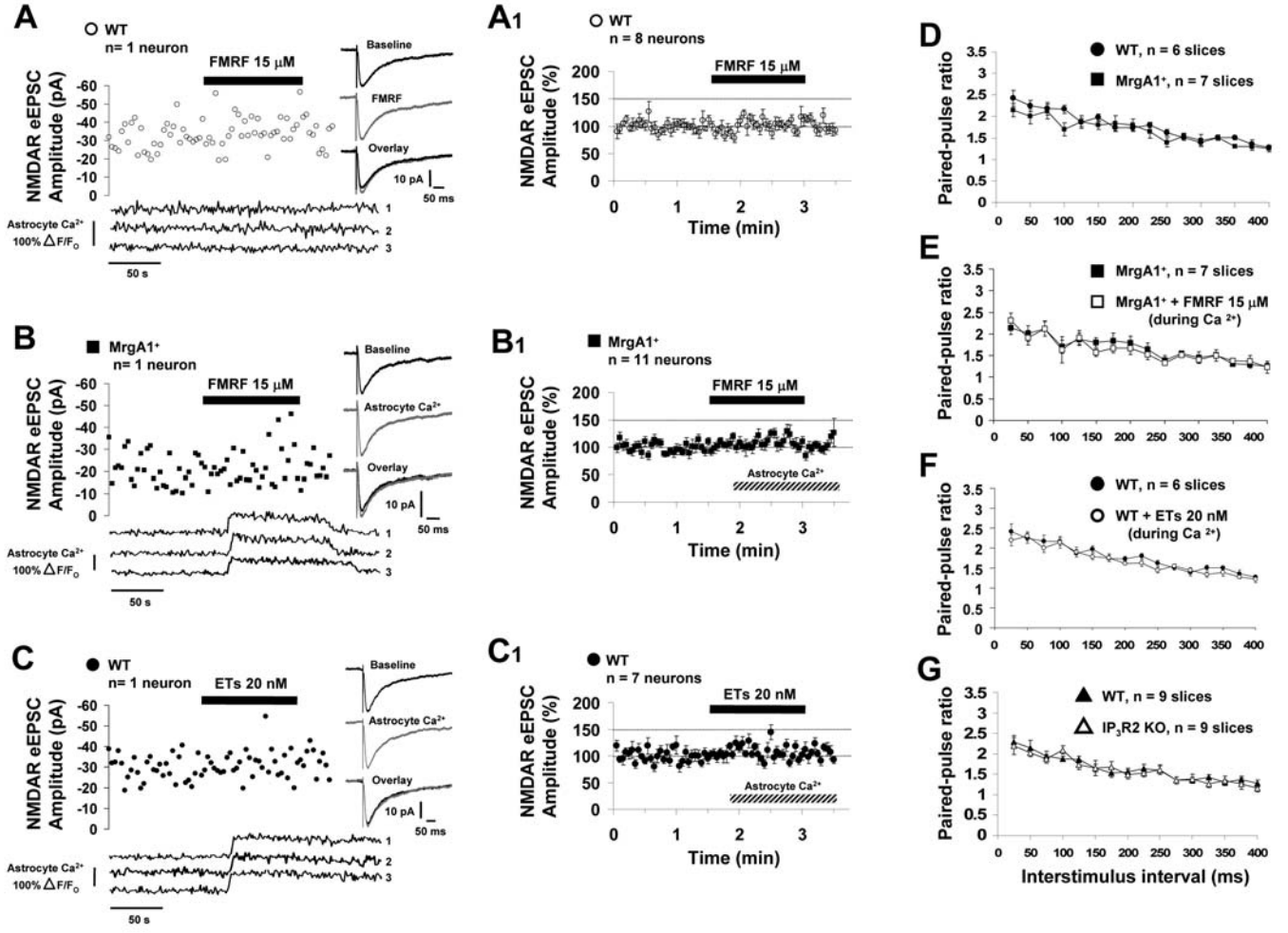

Fig. 2. Astrocytic G_q GPCR Ca^{2+} signaling does not modulate the NMDA eEPSC peak amplitude or PPF in CA1 pyramidal neurons. (**A** and **A1**) WT astrocytes were not activated by FMRF [(A) lower Ca^{2+} traces from three astrocytes surrounding recorded neuron]. FMRF did not nonspecifically affect NMDA eEPSC peak amplitude in WT mice. Representative example (A) and pooled data (A1). (**B**, **B1**, **C**, and **C1**) Activation of $MrgA1^+$ (B and B1) or WT astrocytes (C and C1) by FMRF or ETs, respectively, did not affect NMDA eEPSC peak amplitude. (**D**) MrgA1R expression in astrocytes of $MrgA1^+$ mice did not have a nonspecific effect on PPF ratio compared with WT littermate mice. (**E** and **F**) PPF ratios in $MrgA1^+$ slices before (solid squares) and during (open squares) FMRF-evoked astrocyte Ca^{2+} elevations (E) or in WT slices before (solid circles) and during (open circles) ET-evoked astrocyte Ca^{2+} increases (F) were not significantly different. (**G**) PPF is not altered in IP_3R2 KO mice compared with WT littermate control mice.

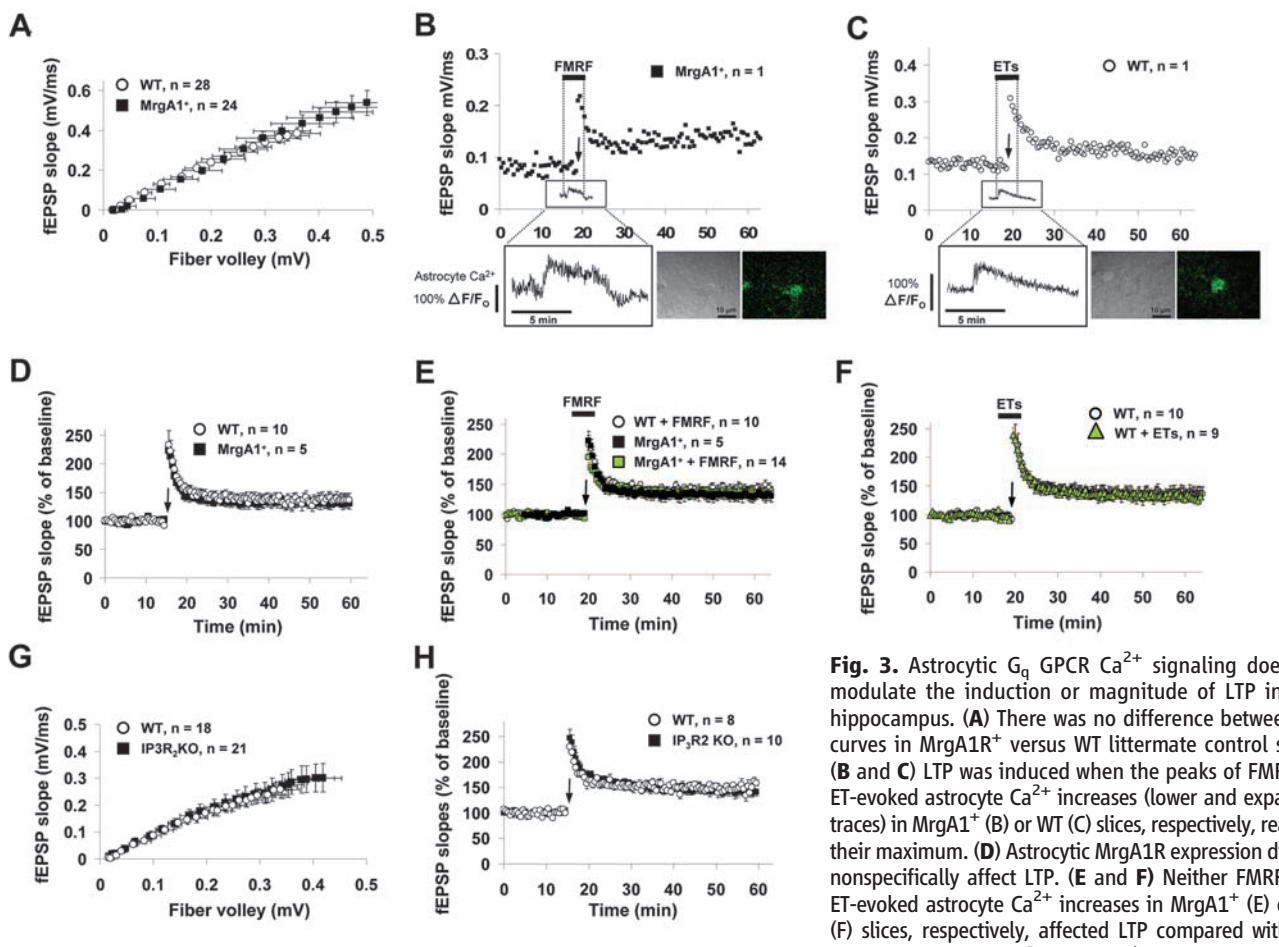

Fig. 3. Astrocytic G_q GPCR Ca^{2+} signaling does not modulate the induction or magnitude of LTP in CA1 hippocampus. (**A**) There was no difference between I/O curves in MrgA1R$^+$ versus WT littermate control slices. (**B** and **C**) LTP was induced when the peaks of FMRF- or ET-evoked astrocyte Ca^{2+} increases (lower and expanded traces) in MrgA1$^+$ (B) or WT (C) slices, respectively, reached their maximum. (**D**) Astrocytic MrgA1R expression did not nonspecifically affect LTP. (**E** and **F**) Neither FMRF- nor ET-evoked astrocyte Ca^{2+} increases in MrgA1$^+$ (E) or WT (F) slices, respectively, affected LTP compared with two sets of control slices [(E), MrgA1$^+$ slices without FMRF application, WT littermate slices with FMRF application; (F), WT slices without ET application]. (**G** and **H**) I/O curves (G) and LTP (H) in IP_3R2 KO mice are not affected compared with WT littermate control mice. Arrows indicate LTP induction (2 × 100 Hz).

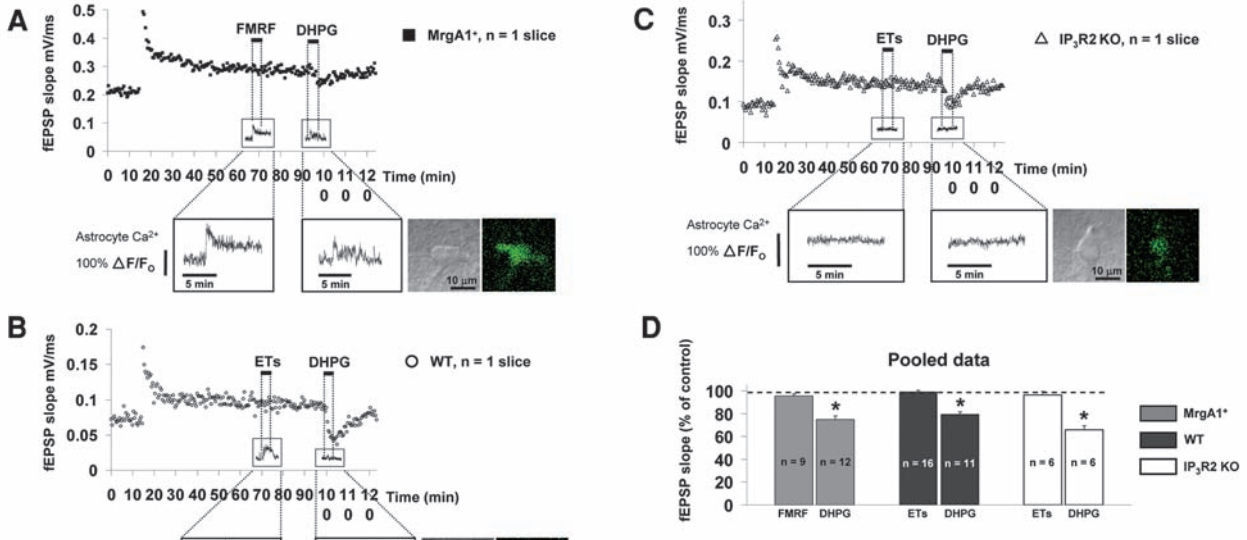

Fig. 4. Astrocytic G_q GPCR Ca^{2+} signaling does not modulate the maintenance of LTP (2 × 100 Hz) in CA1 hippocampus. (**A** and **B**) Neither FMRF- nor ET-evoked astrocyte Ca^{2+} increases (lower and expanded traces) in MrgA1$^+$ slices (A) or WT slices (B), respectively, modulated the maintenance of LTP. As a control for modulation of LTP maintenance, DHPG (50 μM) was applied. (**C**) ETs and DHPG did not evoke any astrocyte Ca^{2+} increases in IP_3R2 KO slices. Whereas ETs did not modulate the maintenance of LTP, DHPG induced a clear depotentiation independent of astrocyte Ca^{2+} elevations. (**D**) Summary histogram showing that DHPG, but not FMRF or ETs, affected the maintenance of LTP in MrgA1$^+$, WT, or IP_3R2 KO slices. Asterisks indicate statistical significance ($P < 0.0001$).

0.0001; Fig. 4, B and D; WT, 79.54 ± 2.03%, n = 11, $P < 0.0001$). To address the possibility that the DHPG-mediated depotentiation could be due in part to astrocyte Ca^{2+}, we performed the same experiments using IP_3R2 KO mice. The magnitude of DHPG-induced depotentiation in IP_3R2 KO slices was not only significant ($P < 0.0001$), it was also similar to the magnitude of depotentiation that was recorded in WT littermate slices ($P = 0.43$), indicating that depotentiation does not rely, even in part, on Ca^{2+}-dependent gliotransmitter release from astrocytes (Fig. 4, C and D; IP_3R2 KO, 66.95 ± 2.79%, n = 6; WT, 72.70 ± 5.72%, n = 8). These results demonstrate and confirm previous data that DHPG-induced modulation of neuronal activity (*28*, *29*), such as depotentiation (*26*), is due to the direct action of DHPG on neuronal group I mGluRs (*26*), and not to astrocytic group I mGluR-mediated Ca^{2+} elevations and putative gliotransmitter release.

We provide here strong evidence that G_q GPCR Ca^{2+} signaling in astrocytes does not affect spontaneous and evoked excitatory action potential (AP)-mediated synaptic transmission or short- and long-term plasticity at the SC-CA1 synapse. We used two molecular tools (the $MrgA1^+$ and IP_3R2 KO mouse models), as well as the activation of endogenous astrocytic G_q GPCRs, to manipulate Ca^{2+} in astrocytes. A battery of eight electrophysiological protocols (sEPSCs, NMDA eEPSCs, evoked AMPA fEPSPs, I/O curves, PPF, PTP, and two forms of LTP) were studied, all of which point to a lack of modulation of excitatory AP-mediated synaptic transmission by astrocytic G_q GPCR Ca^{2+} signaling. The most logical conclusion from the present analysis is that astrocytic G_q GPCRs and Ca^{2+} signaling activity are not tied to the release of gliotransmitters affecting synaptic transmission or short and long-term plasticity. Therefore, our results suggest that gliotransmission reflects the pharmacological approaches that were used in previous studies (*3*–*10*, *12*) and, at least within the hippocampus, does not occur when the endogenous regulators of astrocyte Ca^{2+}, the G_q GPCRs, or the IP_3R2 themselves are stimulated or inactivated in a cellular-selective manner. These findings suggest that the mechanisms of gliotransmitter release should be reconsidered. These results have profound implications for our understanding of synaptic transmission and should affect the interpretation of a broad range of findings. Thus, the purpose of neuron-to-astrocyte G_q GPCR Ca^{2+} signaling in neurophysiology remains an open question.

References and Notes

1. X. Wang *et al.*, *Nat. Neurosci.* **9**, 816 (2006).
2. J. T. Porter, K. D. McCarthy, *J. Neurosci.* **16**, 5073 (1996).
3. M. C. Angulo, A. S. Kozlov, S. Charpak, E. Audinat, *J. Neurosci.* **24**, 6920 (2004).
4. T. Fellin *et al.*, *Neuron* **43**, 729 (2004).
5. C. J. Lee *et al.*, *J. Physiol.* **581**, 1057 (2007).
6. M. Navarrete, A. Araque, *Neuron* **57**, 883 (2008).
7. L. Pasti, A. Volterra, T. Pozzan, G. Carmignoto, *J. Neurosci.* **17**, 7817 (1997).
8. G. Perea, A. Araque, *J. Neurosci.* **25**, 2192 (2005).
9. E. Shigetomi, D. N. Bowser, M. V. Sofroniew, B. S. Khakh, *J. Neurosci.* **28**, 6659 (2008).
10. G. Perea, A. Araque, *Science* **317**, 1083 (2007).
11. A. Serrano, N. Haddjeri, J. C. Lacaille, R. Robitaille, *J. Neurosci.* **26**, 5370 (2006).
12. C. Agulhon *et al.*, *Neuron* **59**, 932 (2008).
13. T. A. Fiacco *et al.*, *Neuron* **54**, 611 (2007).
14. T. A. Fiacco, C. Agulhon, K. D. McCarthy, *Annu. Rev. Pharmacol. Toxicol.* **49**, 151 (2009).
15. N. X. Tritsch, D. E. Bergles, *Neuron* **54**, 497 (2007).
16. J. Petravicz, T. A. Fiacco, K. D. McCarthy, *J. Neurosci.* **28**, 4967 (2008).
17. X. Li, A. V. Zima, F. Sheikh, L. A. Blatter, J. Chen, *Circ. Res.* **96**, 1274 (2005).
18. Y. Sasaki *et al.*, *J. Neurochem.* **68**, 2194 (1997).
19. M. Andersson, F. Blomstrand, E. Hanse, *J. Physiol.* **585**, 843 (2007).
20. T. A. Fiacco, K. D. McCarthy, *J. Neurosci.* **24**, 722 (2004).
21. O. Pascual *et al.*, *Science* **310**, 113 (2005).
22. R. S. Zucker, *Neuron* **17**, 1049 (1996).
23. H. J. Chung *et al.*, *Proc. Natl. Acad. Sci. U.S.A.* **106**, 635 (2009).
24. C. C. Huang, Y. C. Liang, K. S. Hsu, *J. Biol. Chem.* **276**, 48108 (2001).
25. R. Li, F. S. Huang, A. K. Abbas, H. Wigström, *BMC Neurosci.* **8**, 55 (2007).
26. W. M. Zho, J. L. You, C. C. Huang, K. S. Hsu, *J. Neurosci.* **22**, 8838 (2002).
27. Y. Izumi, C. F. Zorumski, *J. Neurosci.* **28**, 9557 (2008).
28. G. Mannaioni, M. J. Marino, O. Valenti, S. F. Traynelis, P. J. Conn, *J. Neurosci.* **21**, 5925 (2001).
29. M. G. Rae, A. J. Irving, *Neuropharmacology* **46**, 1057 (2004).

30. We thank K. Casper for making $MrgA1^+$ mice; J. Chen for providing IP_3R2 KO mice; and B. Djukic, B. Philpot, A. Roberts, and J. de Marchena for valuable help and discussions. This work was supported by NIH grants NS033938 and NS020212.

Supporting Online Material

www.sciencemag.org/cgi/content/full/327/5970/1250/DC1
Materials and Methods
SOM Text S1 to S14
Figs. S1 to S3
References
Movie S1

17 November 2009; accepted 19 January 2010
10.1126/science.1184821

RTEL-1 Enforces Meiotic Crossover Interference and Homeostasis

Jillian L. Youds,[1] David G. Mets,[2] Michael J. McIlwraith,[3] Julie S. Martin,[1] Jordan D. Ward,[1]* Nigel J. ONeil,[4] Ann M. Rose,[4] Stephen C. West,[3] Barbara J. Meyer,[2] Simon J. Boulton[1]†

Meiotic crossovers (COs) are tightly regulated to ensure that COs on the same chromosome are distributed far apart (crossover interference, COI) and that at least one CO is formed per homolog pair (CO homeostasis). CO formation is controlled in part during meiotic double-strand break (DSB) creation in *Caenorhabditis elegans*, but a second level of control must also exist because meiotic DSBs outnumber COs. We show that the anti-recombinase RTEL-1 is required to prevent excess meiotic COs, probably by promoting meiotic synthesis-dependent strand annealing. Two distinct classes of meiotic COs are increased in *rtel-1* mutants, and COI and homeostasis are compromised. We propose that RTEL-1 implements the second level of CO control by promoting noncrossovers.

Homologous recombination repair of meiotic DNA double-strand breaks (DSBs) is regulated to ensure the correct number and placement of meiotic crossovers (COs). One CO per chromosome ensures that homologous chromosomes are held together, can orient toward opposite spindle poles, and thereby segregate correctly at the first meiotic division. Crossover interference (COI) ensures appropriate distribution of COs among chromosomes because the formation of one CO reduces the likelihood of other COs occurring nearby. Meiotic COI is "complete" in *Caenorhabditis elegans*: Only a single CO occurs on each chromosome (*1*, *2*). COI is regulated in part by the condensin I complex, which limits meiotic DSB formation (*3*). Because the average number of meiotic DSBs per chromosome is 2.1 (*3*), and only one of these is repaired as a CO, a second tier of CO control must exist downstream of meiotic DSB formation that channels about half of all DSBs into noncrossovers (NCOs). However, the proteins involved in generating a meiotic CO versus NCO are not well understood.

Human RTEL1 (and *C. elegans* RTEL-1, by homology) negatively regulates recombination by disassembling D loop–recombination intermediates during DNA repair (*4*). If RTEL1 acts similarly on meiotic recombination intermediates, it could be the key protein required to execute NCOs by promoting meiotic synthesis-dependent strand annealing (SDSA). By genetic measurements, recombination in *C. elegans rtel-1* mutants was significantly increased in five genetic intervals on three chromosomes, including both chromosome center and arm regions (Fig. 1A and table S1)

[1]DNA Damage Response Laboratory, London Research Institute, Cancer Research UK, Clare Hall, South Mimms, EN6 3LD, UK. [2]Howard Hughes Medical Institute, Department of Molecular and Cell Biology, University of California at Berkeley, Berkeley, CA 97420, USA. [3]Genetic Recombination Laboratory, London Research Institute, Cancer Research UK, Clare Hall, South Mimms, EN6 3LD, UK. [4]Department of Medical Genetics, Faculty of Medicine, University of British Columbia, Vancouver, BC, V6T 1Z4, Canada.

*Present address: Department of Cellular and Molecular Pharmacology, University of California, San Francisco, San Francisco, CA, 94518–2517, USA.
†To whom correspondence should be addressed. E-mail: simon.boulton@cancer.org.uk